Microscopic Illustration of Zinc evaporation and ZnO nanowire production during brass alloy sintering

[1] A. Behvar, [2] H. Eftekhary, [3] A. Cheraghi, [4] M. Adazbeh
Corresponding author, Sharif University of Technology, Material science department,
Email address: alireza.behvar@gmail.com
Phone: +98 911 987 5436
Sharif University of Technology, Material science department,
Email address: hosnaeftekhary@gmail.com
Sharif University of Technology, Material science department,
Email address: alireza.cheraghi.86@gmail.com,
Sahand University of technology, Metallurgy department,
Email address: azadbe@sut.ac.ir

Abstract - One of the basic problems in sintering process of brass powder metallurgy components is the evaporationof zinc.In order to preserve the Zn content inexpensive experiments and methodshave been employed. In the current study, zinc lossis prevented and precipitation of zinc is achieved by formation of ZnO nanoparticles.Under Argon and Nitrogen atmosphere, the zinc vapor was grown in ZnO format on the copper heterogeneous catalyst.The catalyst is less oxidized due to zinc oxidation in the boundary layer of Zn-Cu powder particles. Zinc vapor exits more quickly from the powder sample than pressed sample and nanoparticles of ZnO are formed in a short time. It is evident that zinc evaporation is tougher from a more homogeneous and pressed sample, due to closure of gas exit path. To explore the mentioned matter, a pressed sample containing a groove was subjected to similar experiment conditions. It was observed that the nanoparticles which were formed on the grooved pressed sample are more than those formed from not grooved sample and less from powdered sample.While thecontrolling mechanism of the evaporation is diffusion, boundary layer is the controlling mechanismof the formation of zinc oxide nanoparticles.Moreover, the X-Ray diffraction pattern and Scanning Electron Microscopy results depict [101] as the preferable growth orientation of zinc oxide nanoparticles.

Keywords: zinc evaporation, zinc oxide nanoparticles, boundary layer, SEM, XRD

1. Introduction

Due to high mechanical properties as well as high corrosion resistance, brass alloys are utilized widely in industrial products [1,2]. Alpha brass, containing 20-36 % zinc, is a highly used type of brasses [3]. High zinc pressure at sintering temperatures results in zinc evaporation and consequently, dropping mechanical properties and chemical composition change [4,5]. To reduce thedegrading effects of zinc evaporation, pre-alloyed Cu-Zn powders have been employed instead of copper and zinc powder mixture [6]. Although zinc evaporation decreases by pre-alloyed powders application, evaporation does not disappear thoroughly. The sintering temperature is of great importance and the optimum temperaturein which the least evaporation occursis reported to be in the range of1088-1198 K [6]. Employing alumina or graphite coverage on samples, the weight lossis 1-2% in the mentioned temperature range[4,5].

The importance of ZnO nanoparticles' application in optoelectronics has made an extensive development in ZnO nanoparticle production in recent years [7]. Several methods have been proposed for the production; electrodepositing [8], decomposition from solution [9] and aerosol process [10]. Physical vapor decomposition is another method, with high repeatability, used in ZnO nano-wire production [11]. The process involves material evaporation, transfer and precipitation on surface. The resulted structure possessesrodsin which therod diameter depends on production parameters such as temperature, pressure and gas flow [12].

Brass sintering along with ZnO nano-structure production in tube furnace is studied simultaneously in this investigation. The zinc evaporation is proved in macroscopic scale and the formation condition is investigated. Additionally, the effects of heterogeneous copper catalyst as well asargon and nitrogen atmosphere on ZnO nanoparticles formation are probed in this study.

2. Materials and Methods

Regarding previous research, the materials used were chosen as brass alloyed powder with Cu-28%Zn composition [13,14]. Prepared by water atomization method, the powder was stirred at 65 RPM with 75 wt% lithium stearate for 20 minutes. Cubic samples of powders with 55×10×10 mm^3 dimensions and 7.6-7.8 $g.cm^{-3}$ densities were made under 600 MPa pressure. The pressed samples were sintered in a three-zone tube furnace under Ar and N_2 atmosphere with 2 $liter.min^{-1}$ flow rate. Although the optimum sintering condition is reported to be 1146 K and 45 minutes [14], higher temperatures were also investigated to explore ZnO formation.In order to recover zinc evaporates from the sintering step, the copper catalyst was subjected to outgoing gas at temperatures lower than that of sintering (573-973 K) and zinc is precipitated as ZnO on the catalyst. To prevent catalyst and samples' surfaces from being oxidized, a graphite boat was placed on the gas entrance of the furnace and 15-20 centimeters before brass samples.

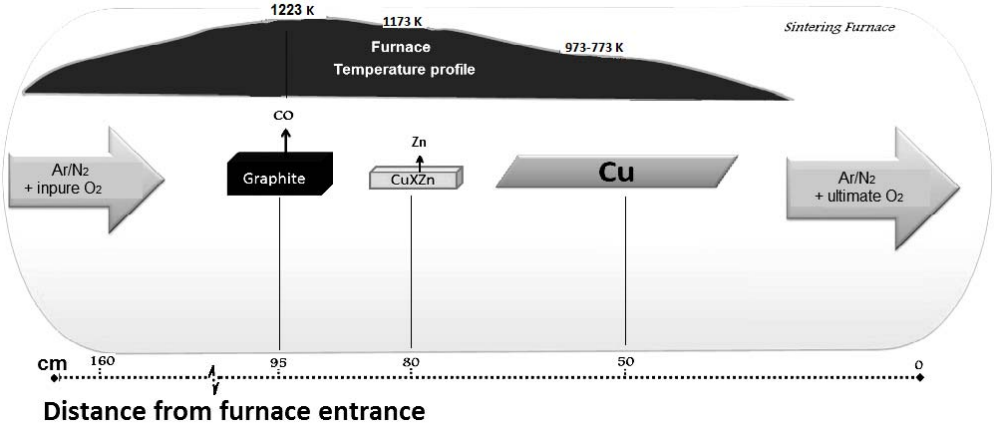

Figure1. Schematic illustration of the process

CO, which is a reductive gas, is formed at high temperatures in presence of graphite based on Boudouard equilibrium curves [16] andprotects copper catalyst surface from oxidizing and preserves the preferred sites for ZnO precipitation.The sintered samples were located in alumina boat in the furnace in two various shapes; powder and segment. The schematic samples' location in the furnace as well as temperature profile and distance from the furnace entrance are shown in figure 1.To prepare catalyst surface, the copper sheets were cut on the edge and sanded perpendicular to the gas flow. The grooves were cleaned by acetone to preserve the preferable sites of superficial adsorption from contamination. Besides, some barriers were made on copper surface to create reverse flow against the gas flow. This increases the contact between the copper surface andthe boundary layer of protective gas furnace.Since the protective gas is impure and has some oxygen content, the zinc vapor oxidizes in the boundary layer and is adsorbed as ZnO on catalyst surface.In order to explore the optimized condition to precipitate nanoparticles of ZnO by in situ method, the experiments were designed with four variables: gas flow rate, gas protective type, temperature and time. XRD was employed to measure the size of the grains and the crystallites. The field emission scanning electron microscope was used to determine the precise size of nanoparticles. Fixing a thermocouple on the samples, the ZnO formation temperature was measured.

3. Results

3.1. Effective mechanisms in zinc vapor precipitation

3.1.1. Fluid boundary layer

Zone 1 in figure 2 depicts part of copper catalyst surface in which zinc oxide precipitates on. In certain range (zone 1) which copper takes the role of catalyst, ZnO is formed and copper is remained unchanged at the end of reactions, due to catalytic role.

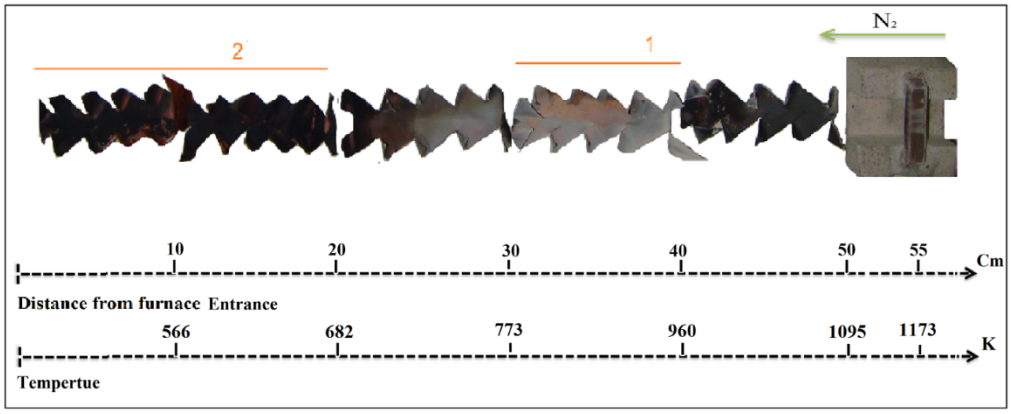

Figure2.Embedding location of specimen and catalyst

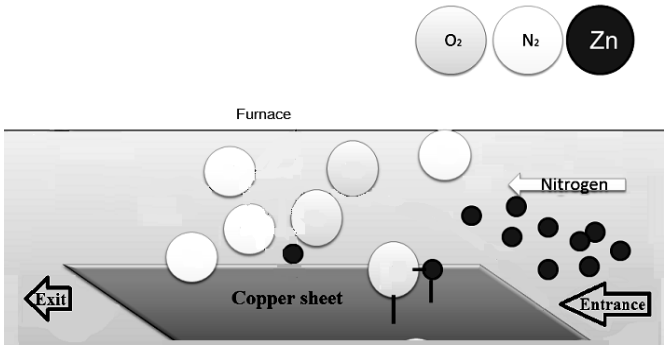

Figure 3. Schematic illustration mechanism of the fluid boundary layer during ZnO particle formation

Temperature drop in boundary layer and favorable conditions to form ZnOare the causes of no oxidization in zone 1. The zinc vapor reacts quickly with the presentedoxygen in the furnace atmosphere and precipitates as ZnO on the copper surface and prevents the copper from oxidation. The existed mechanism in the boundary layer was kind of convection.Diffusing zinc vapor as well as oxygen atoms to the boundary layer, they slow down and because of favorable temperature drop, they react and the product adsorbs on copper surface. Figure 3 shows the mechanism schematically.

Regarding the latter discussion, one of effective parameters in ZnO nanoparticles production is fluid boundary layer which is a function of gas temperature, gas type and surfaces' shapes in contact with gases. Zinc vapor production source is noteworthy in kineticallydiscussion of the process; in the case that the zinc vapors production delays considerably or the mass of the clusters production is low, catalyst surface oxidizes and ZnO nanoparticles production ceases, due to oxygen presence.

3.1.2. Zinc evaporation from brass

Since the pre-alloyed powders of Cu-28%Zn are produced through water atomization technique, it could be assumed that solidification has been completed with complete mixing in liquid and without diffusion in solid [15]. Therefore, external layer of liquid is solidified in non-equilibriumcondition and zinc is pushed back to the powder center at the beginning of solidification. In other words, the powder centers are rich of zinc. According to Scheil equations [17], zinc is pushed back to the grain boundaries and it could be concluded that powder grain boundaries are rich of zinc. Comparing to other areas, grain boundaries have lower melting point and they begin to melt sooner while sintering. As a result, the zinc escape is more severe at the grain boundaries and the holes are formed in the middle of powders in the first steps of sintering. As the sintering progresses, the holes move from grain boundaries towards powders' boundaries. Figure 4 schematically shows the process.

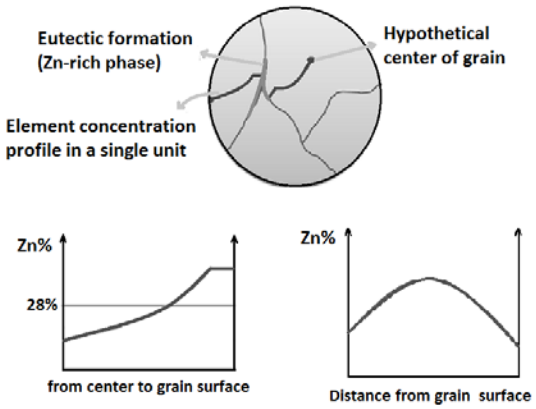

Figure 4. Zn distribution in grains and particles

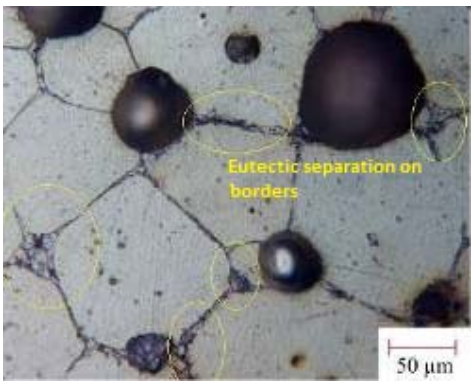

Figure 5. Eutectic separation in boundaries due to Scheil mechanism

Further sintering and solidification result in rearrangement of grains and repetition of the latter process and finally, the pores lie on new boundaries. Figure 5 depicts necklaces configuration of eutectic segregation which is the result of non-equilibrium solidification of powders.Comparing zinc oxide content in powder sample and pressed sample at similar thermodynamic conditions, it is evident that ZnO content, ZnO formation span and also catalyst surface behaviors differ in each sample. Figures 6 and 7 show nanoparticles formed in two cases after 60 minutes andat 1173 K and 2 liters.min^{-1} argon flow rate. As can be seen, nanoparticlesformed from powdered sample have started formation sooner and have higher amount than those formed from pressed sample.

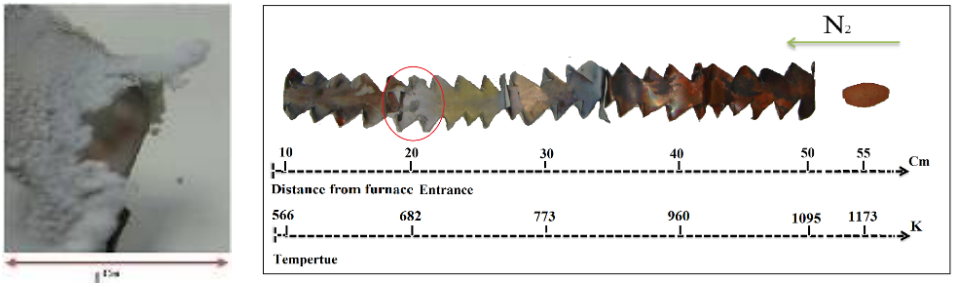

Figure6. Nano particles formed from Zn evaporates of Cu-28%Zn powder formed in 1173 K after 60 minutes.

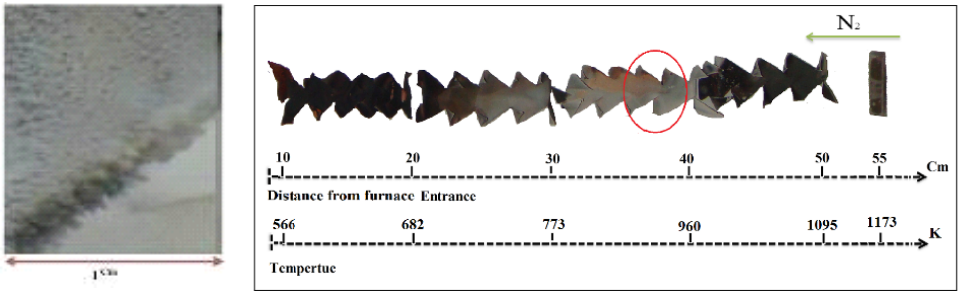

Figure7. Nano particles formed from evaporations of sintered sample after remaining for 60 minutes in 1173 K.

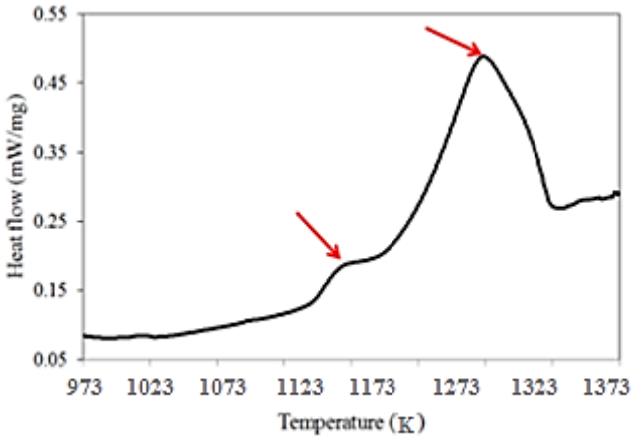

Figure8. Differential Calorimetry results of Cu- 28%Zn powder [13, 6].

It could be inferred thatwhen the liquid phase formed, zinc atoms have gone away through free paths from sample. Hence, zinc atoms exit and consequently pore growth can be assumed as diffusion process. A more precise look at catalyst surface reveals that in the experimentemployingthe powdered sample, the catalyst is less oxidized: since the zinc vapor exits the powdered sample sooner, zinc oxidation in the boundary layer occurs more quickly and copper is less oxidized accordingly.

3.2. Optimized condition to precipitate zinc vapor as oxidized nanoparticles

3.2.1. Sintering temperature effect

Regarding as-received powder's DifferentialScanning Calorimetry diagram, the temperature range of 1193-1203 K is appropriate for cloudy appearance of ZnO formation (figure 8). As can be seen in figure 8, an endothermic reaction has started at about 1153 Kthat could be the result of sudden increase in zinc evaporation. Since 1180 Kis the zinc boiling point, vapor pressure increases dramatically at upper temperatures and all the zinc content in the powder evaporates at upper temperatures. Although it could be concluded that maximum ZnO production occurs at higher temperatures, mechanical properties' degradation is inevitable.

3.2.2. Atmosphere type

Compared to nitrogen atmosphere, argon atmosphere results in three-times smaller ZnO nanoparticles' quantityand lessmacroscopic needle-like structure(figures 9 and 10).

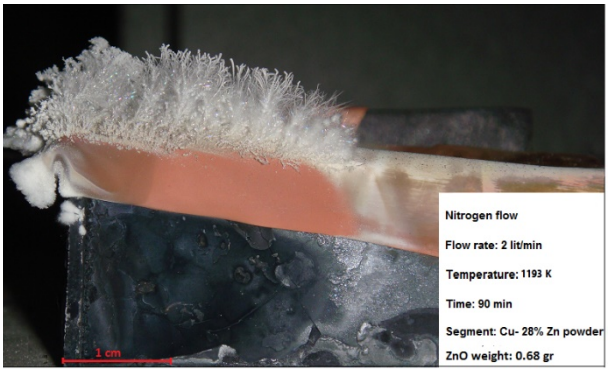

Figure 9. Zinc oxide precipitated in Nitrogen atmosphere.

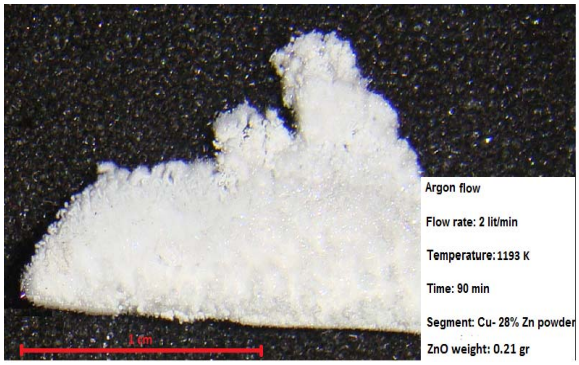

Figure10. Zinc oxide precipitated in Argon atmosphere.

In high temperature (1073 K) and 1atm pressure, the density of argon and nitrogen are 0.487 $g.lit^{-1}$ and 0.308 $g.lit^{-1}$ respectively [18-19].Since argon has higher density, diffusion to the boundary layer is more difficult. The gas viscosity is affected by temperature and influences the fluid boundary layer.

$$Re = \frac{\rho v L}{\mu} \qquad (1)$$

Where:

Re: Reynolds number

ρ: the density of the fluid

v: the mean velocity

L: characteristic linear dimension

μ: the dynamic viscosity

As equation 2 [20] and equation 3 [21] show, gas viscosity increases with temperature increase, due to an increase in dynamic energy. The fluid density is also related to temperature. All experiments have been carried out at temperatures higher than 1123 K. Additionally, the experiment temperature had been fixed to a constant value during any individual experiment and it could be concluded that the density is only a function of gas type during any experiment. Since characteristic linear dimension and gas velocity are fixed to constant values, the density and viscosity of gas should change so that the Reynolds number does not go beyond the critical value to maintain laminar flow. As argon density is higher than that of nitrogen and also argon viscosity is lower than nitrogen viscosity [20] and equations 2 and 3 show, the laminar flow created on catalyzer by argon is wider than that of nitrogen. In fact, argon is heavier and covers a more extensive surface and results in a more difficult condition for zinc gas diffusion through boundary layer and cluster formation. The result is deposition of less amount of zinc as ZnO and difficulty in crystal nuclei growth. Figure 11 shows the schematicboundary layer of two fluids.

$$\mu = 2.67 \times 10^{-5} \frac{\sqrt{M.T}}{\sigma^2.\Omega} \qquad (2)$$

$\mu: gas\ viscosity, poise$

$M: molecular\ weight, grams$

$T: absolute\ temperature\ , K$

$\sigma: collision\ diameter, Angstrom$

$\Omega: collision\ integral$

Sutherland's formula (3)

$\mu = \mu_o \times (a/b) \times (T/To)^{3/2}$

$a = 0.555T_o + C$

$b = 0.555T + C$

μ = *viscosity in centipoise at input temperature T*

μ_o = *reference viscosity in centipoise at reference temperature* T_o

T = *input temperature in degrees Rankine*

T_o = reference temperature in degrees Rankine

C = Sutherland's constant

As result of calculation : in Temperature =1000 K, viscosity of Ar and N_2 is 0.0342 CP and 0.040 CP

3.2.3. Gas Flow Rate

Gas flow rate is an effective parameter in the shape of the boundary layer and an increase in gas flow rate results in shrinking the laminar region. Due to increase in atoms' kinetic energy and collision with gaseous zinc atoms, increase in gas flow rate leads to postponing ZnO formation and ZnO is formed further from sintering zone.As a result of lack of diffusion time, a great deal of zinc vapor moves along with turbulent flow and exits the furnace.Since the catalyst surface is covered with laminar gas flow and gaseous zinc atoms do not have sufficient kinetic energy at low flow rates, diffusion in boundary layer is not complete and clusters are not formed properly. As can be seen in figure 12, nanoparticles' formation zone is different from sintering zone (gaseous ZnO formation zone).

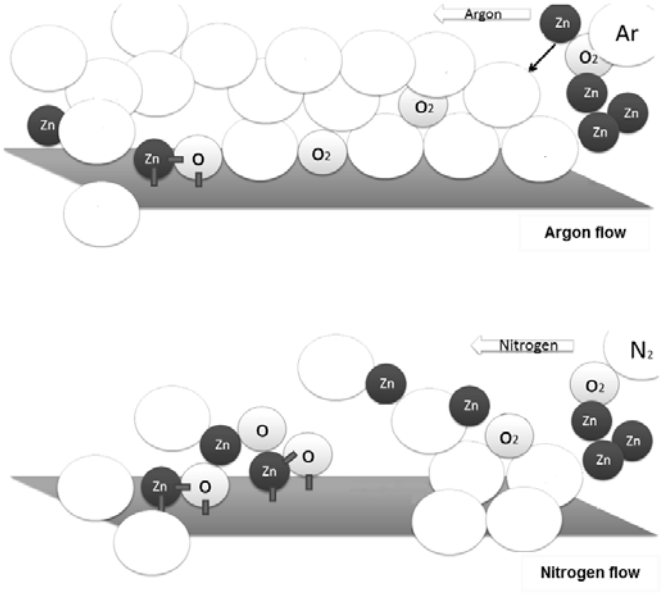

Figure11. Schematic image of fluid layer in Argon and Nitrogen atmosphere.

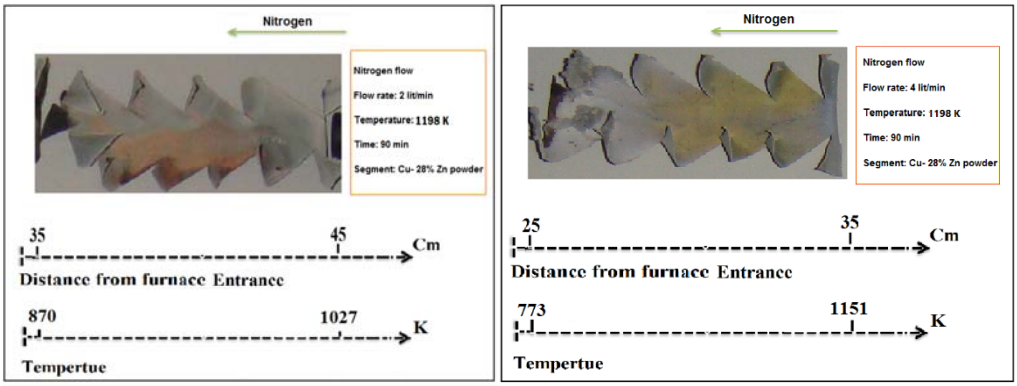

Figure12. Gas flow effect on shifting Zn vapor precipitation site.

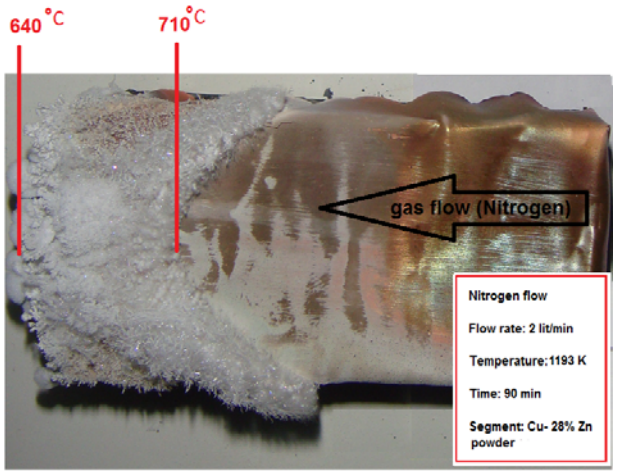

Figure 13. Condensation temperature range of ZnO nanoparticles.

3.2.4. Condensationzone Temperature

The condensation zone temperature is relevant to atmosphere gas type and gas flow rate. A more precise look at nanoparticles' formation zone in figure 13 reveals the temperature profile on the catalyst surface. In addition to the condensation zone temperature, the empirical profile shows critical temperature required for crystallite nucleation on the surface. Since the temperature of this zone is a function of experimental parameters, the condensation zone temperature achieved is different. However, the results show that condensation zone has started from 983 K in nitrogen atmosphere (figure 13).

3.3. ZnO Nanoparticles Analysis

3.3.1. Preferable Crystalline Planes

Figure 14 shows the XRD of the white particles (ZnO) formed on copper catalyst surface from pressed sample at 1193 K, 90 minutes and 2 lit.min^{-1} argon flow rate. The spectrum shows a polycrystalline structure. The peaks arising from (101), (100), (002), (102) and (110) planes which are relevant to ZnO hexagonal structure are clearly evident in all samples.As can be seen, the peak intensity ratio of (101) diffractionis higher than other planes. In other words, the preferableorientation of hexagonal structure growth [101].

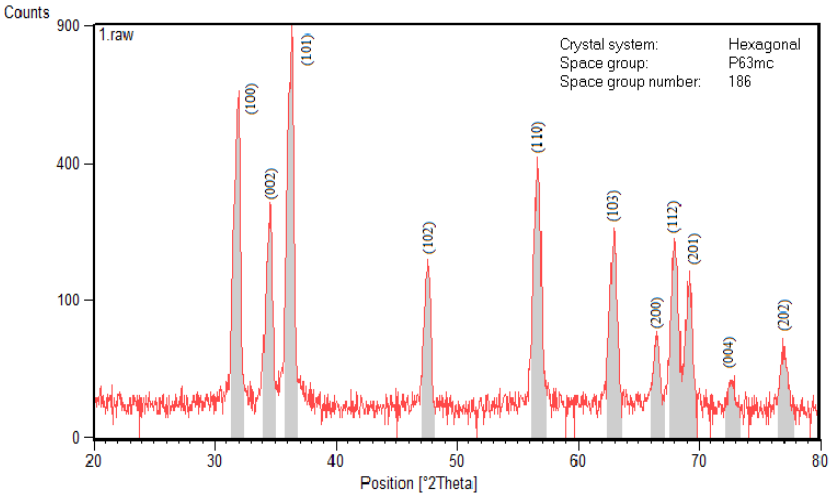

Figure 14. X-Ray diffraction diagram of ZnO nanorods on a compressed specimen in Argon atmosphere flowing in 2 Liter/min, 90minutes in 1193 K.

3.3.2. Nanorods Morphology

ZnO hexagonal nanorods can be clearly observed in the samples' SEM images (Figure 15). As can be seen, nanorods are formed on micro rods which seem like whiskers. According to the results,increase in catalyst surface exposure to furnace atmosphere leads the growth of the primary nanorods nuclei to blades with micron dimensions. New hexagonal nanorods repeatedly nucleate on blades and this cycle continues and consequently, single crystals of blades are remained. Further study reveals a dendrite like growth in blades and secondary arms are formed on preliminary ones. Figure 16.a shows a dense mass of nuclei in various directions which are formed on some blades' intersection. The same nanorods with higher resolution can be seen in figure 16.b. and hexagonal like structure of nanorod is evident in this image. As figure 16 shows, small nuclei have nucleated on thick blades and they will grow in preferableorientations andhexagonal structures will be constructed. The reason in which the hexagonal rods switch to cylinder or blades is the existence of different preferable growth orientations.XRD pattern demonstrates that the preferable growth orientations are [101], [100], [002], [102] and [110] (figure 16) and nano ZnO has been precipitated in773-973 K range. Because of cylindrical temperature profile and radial heat transfer towards the center, nanoparticles' growth has been possible in all mentioned orientations. First, the growth in [101] has had higher rate than other orientations and a hexagonal structure has been constructed. Then and over the time, nanoparticles have grown towards furnace temperature profile (cylindrical furnace center axis) and growth in [101] orientation has slowed down. Consequently, growth in other orientations has speeded up and nanorods' structure has changed from hexagonal to cylinder or blade (figure 16).

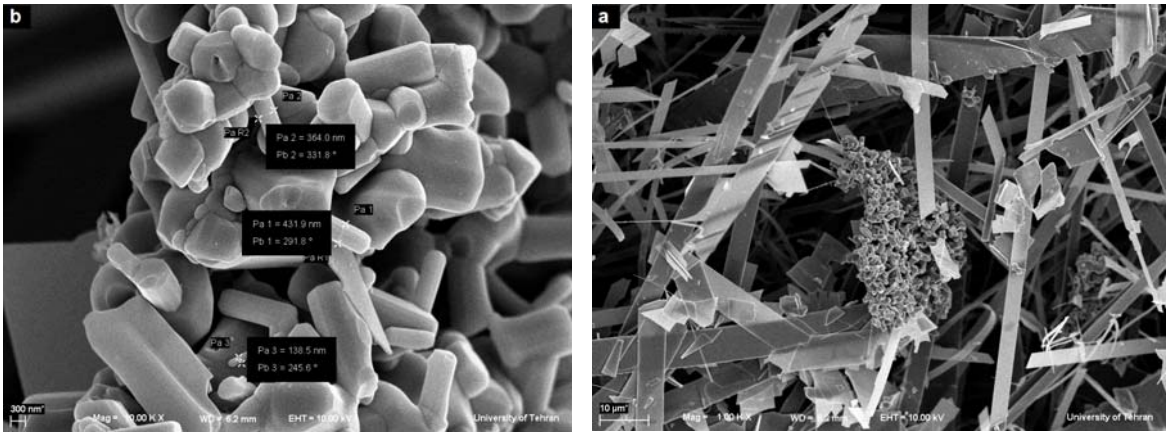

Figure 15. FESEM results of 700 nm ZnO nanorods. a) a cluster of nanorod nuclei, b) Magnification of hexagonal nanorods

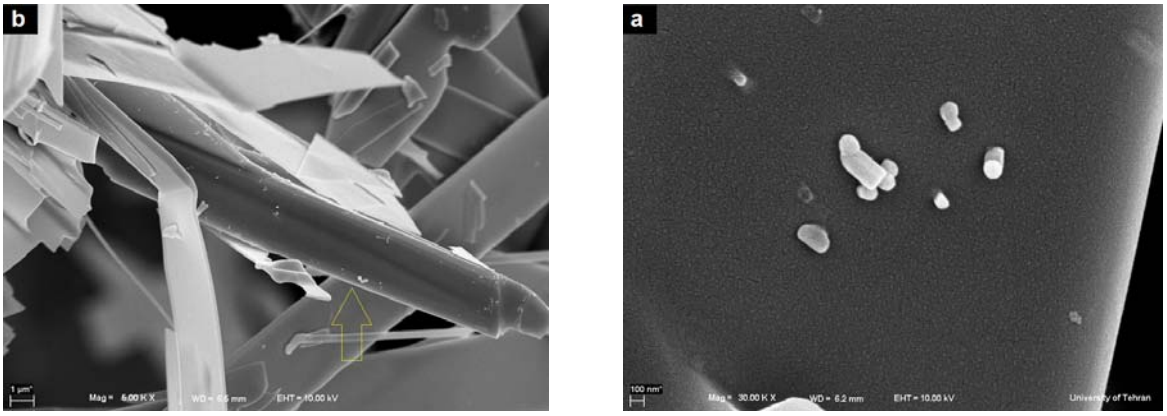

Figure 16. Grown hexagon turned into a cylinder shaped rod. 100 nm hexagons formed on grown super rods.

4. Discussion

It is macroscopically showed that zinc evaporation occurs during sintering from brass alloys. The zinc vapor loss can be prevented by process optimization and precipitating the zinc as nano sized ZnO on copper catalyst. In other words, nano sized ZnO can be achieved using by in situ method and sintering the brass alloys in tube furnace. Additionally, the evaporated zinc is measured by weighing precipitated ZnO and there is no need to use expensive experiments and methods.

Controlling mechanism of zinc evaporation is relevant to diffusion path and the evaporation has direct relationship with temperature and time. The amount of evaporated zinc from a sample containing superficial groove is considerably higher than healthy sample in which is an indicative of evaporation relevance to diffusion path. Boundary layer mechanismcould be controlling over the size of nanoparticles; the nano size ZnO formation at 2 $lit.min^{-1}$ nitrogen atmosphere is feasible at temperatures lower than 983 K. The gas type influences the structure which could be the result of difference between the shape and the thickness of related boundary layers on catalyst.Hence, the physical properties of gas atmosphere have direct impact on the boundary layer and consequently, on ZnO formation.

XRD pattern indicates [101] as the preferable growth orientation of zinc oxide nanoparticles. A dimension range from nanometer to micrometer is observed for nanorods, according to SEM images; the growth of preliminary nanorods over the time and repeated nucleation on grown micro rodsare the causes.

5. References

[1] H. Imai, Y. Kosaka and A. Kojima, "Characteristics of Machinable Lead-Free P/M Brass Alloys With Graphite", Proceeding of 46th Technology Conference of Copper and Copper Alloys, pp. 153-154, 2006.
[2] K. Katsuyoshi, I. Hisashi, U. Junko, K. Yoshiharu and K. Akimichi, "Environmental Benign Brass Alloys Dispersed With Graphite Particles Fabricated Via Solid-State Sintering Process", Transaction of JWRI, Vol. 37, No. 2, 2008.
[3] G. S. Upadhyaya, "Sintered Metallic and Ceramic Materials", John Wiley and Sons, LTD, 2000.
[4] I. D. Radomysel Skii, G. A. Baglyuk and G. E. Mazharova, "Production and Properties of Brass-Base P/M Constructional Materials", Translated from Poroshkovaya Metallurgiya, Vol. 255, No. 2, pp. 56-64, 1986.
[5] Q. Sum, "Zinc Losses During Sintering of Prealloyed Leaded Brass", PM Technology, Vol. 19, No. 3, pp. 175-177, 2001.
[6] A. Mohammadzadeh, M. Azadbeh, A. Sabahi Namin, A. Behvar, M. Dokhantchi,"Modeling and Evaluating of Densification and Impact Energy during Supersolidus Liquid Phase Sintering of Brass Alloyed Powder", The first international and sixth joint conference of Iranian metallurgical engineering society, university of Tehran ,6 -8 December 2012.
[7] Y.W.Heo, D.P. Norton, L.C.Tien, Y.Kwon,B.S.Kang,F.Ren,S.J.Pearton,R.Laroche,Mater. Sci. Eng.R47(2004) 1.
[8] Y.Li, G.W.Meng, L.D.Zhang, F.Phillip, Appl. Phys. Lett. 76(2000)2011. Ordered Semiconductor ZnO Nanowires Arrays and Their Photoluminescence Properties
[9] Esmaeel Darezereshki, Mostafa Alizadeh, Fereshteh Bakhtiari, Mahin Schaffie, Mohammad Ranjbar," A novel thermal decomposition method for the synthesis of ZnO nanoparticles from low concentration ZnSO4 solutions", Applied Clay Science 54 (2011) 107–111.
[10] Beril K.Ozcelik, CelaletdinErgun,"Synthesis of ZnO nanoparticles by an aerosol process",Ceramics International 40 (2014)7107–7116.
[11] E. Comini, C. Baratto, G. Faglia, M. Ferroni, A. Vomiero, G. Sberveglieri, Quasione dimensional metal oxide semiconductors: preparation, characterization and application as chemical sensors, Prog. Mater. Sci. 54 (2009) 1–67.
[12] G. Jimenez-Cadena, E. Comini, M. Ferroni, A. Vomiero, G. Sberveglieri," Synthesis of different ZnO nanostructures by modified PVD process and potential use for 1dye-sensitized solar cells", Materials Chemistry and Physics 124 (2010) 694–698.
[13] A.Mohammadzadeh, M.Azadbeh, A. Sabahi Namin, A.Behvar, M.Dokhantchi," Modeling and Evaluating of Densification and Impact Energy during Supersolidus Liquid Phase Sintering of Brass Alloyed Powder" The first International and the Sixth Joint Conference of Iranian Metallurgical Engineering Society and Iranian Foundrymen's Society, University of Tehran, 6-8 December 2012.
[14] A. Mohammadzadeh, M. Azadbeh, H. Danninger, "New concept in analysis of supersolidus liquid phase sintering of alpha brass", Powder Metallurgy (2014), In press.
[15] M.M. Pariona, C. Bolfarini, R.J. dos Santos, C.S. Kiminami," Application of mathematical simulation and the factorial design method to the optimization of the atomization stage in the spray forming of a Cu-6% Zn alloy", Journal of Materials Processing Technology 102 (2000) 221-229.
[16] M. J. Prins, K. J. Ptasinski, F. J. J. G. Janssen," Thermodynamics of gas-char reactions: first and second low analysis", Chemical Engineering Science 58 (2003) 1003 – 1011.
[17] M. Xiong, A. V. Kuznetsov, "Comparision between Lever and Scheil Rules for Modeling of Microporosity Formation during Solidification", Flow, Turbulence and Combustion 67: 305-323, 2001.
[18] W. J. Little," Tables of Thermodynamic Properties of Argon from 100 to 3000 K", ARO Project No. VT8002, April 1964.
[19] R. T. Jacobsen, R. B. Stewart," Thermodynamic Properties of Nitrogen Including Liquid and Vapor Phases from 63-2000 K with Pressures to 10,000 Bar", J. Phys. Chem. Ref. Data Vol.2 , No.4 , 1973.
[20] Transport Phenomena in Metallurgy; G. H. Geiger, D. R. Poirier, Addison-Wesley Publishing Company, No.75-164648, 1973.
[21] Crane Company. 1988. Flow of fluids through valves, fittings, and pipe. Technical Paper No. 410 (TP 410).